



ISSN 1110-0451

Arab Journal of Nuclear Sciences and Applications

Web site: ajnsa.journals.ekb.eg



(E S N S A)

Characteristics Analysis of Contrast Transfer Images Based on Optoelectronic Integrators

Mohamed S. El_Tokhy, Elsayed H. Ali* and Refaat. M Fikry

Engineering Department, NRC, Atomic Energy Authority, 13759 Cairo, Egypt

ARTICLE INFO

Article history:

Received: 15th Oct. 2020

Accepted: 14th Apr. 2021

Keywords:

Signal to Noise Ratio,
Optical Signal Processing,
Optoelectronic Integrated
Circuits.

ABSTRACT

The present study is concerned with overcoming the resultant image degradation due to the integration of the optoelectronics instruments (OEIDs). Accordingly, the characteristics of the image, due to optoelectronic integration, are handled and improved. The image features include the transmission mechanism and the concentration of electrons. The device performance is improved through the optimal design of the basic parameters. Furthermore, the efficient design of structure parameters will minimize the reabsorption process. Optimization of the integrator structure is realized. MATLAB environment is used for devising this instrument. The optimal number of integrator base and wave number characterizing the scale of near-infrared (NIR) image nonuniformity are estimated to be 13 and 0.206 respectively. The output of this instrument is also conducted through closed-form expressions of the underlined instrument. The achieved results show a remarkable accuracy for handling the deformations raised during the integration process. In addition, the results show that the carrier concentration changes the behavior of the output of the NIR image.

1. INTRODUCTION

Infrared light-emitting diodes (LEDs) have many significant uses, including remote control systems, surveillance cameras, LiFis, and optical communications. In recent years, there has been an increased demand for short-distance optical interconnects (OIs) such as high-speed communications between microprocessors and memory for large data processing[1, 2]. Lately, there has been an increase in interest in optoelectronic integrated devices, which comprise the core in different optical signal processing and optical computing systems[3-5]. Optoelectronic integrated devices (OEIDs), manufactured by the epitaxial integration of optoelectronic products are encouraging optimal communication and optical information processing areas[6-9]. These integrated optoelectronic systems with multi-functions like optical amplification, bi-stability, and switching are exciting in OEICs. In fiber-optic networks, optical switches, and optical computers, the tool is seen as a critical feature[10]. A considerable effort has been made to manufacture and analyze optoelectronic integrated devices (OEID) performance[11]. Heterostructure devices have long been recognized to be used to transform radiation [12].

Besides, imagery products from near-infrared (NIR) have attracted considerable interest because of their potential applications in the fields of protection, night vision, wafer inspections for semiconductors, and medical imaging. A practical alternative to NIR imaging is transforming NIR light into visible light, recognizable with the accessible digital camera or naked eyes. [13]. The most exciting one for infrared imaging applications is an integrated semiconductor up-conversion device. Nevertheless, these devices were built with different materials and structures aimed at specific regions of the wavelength. Besides, these research tools for infrared imaging pixelless have been presented[14].

Over the past two decades, significant progress has been made that has resulted in larger focal plane arrays (FPAs), which are cheaper than HgCdTe sensors, particularly for long-wavelength infrared (LWIR).[15, 16]. An up-conversion system based on integrated devices was proposed and demonstrated several years ago[12]. This unit uses intersubband transitions for middle infrared radiation (MIR) detection and interband transitions for near-infrared radiation (NIR) or visible radiation (VIR) emissions. Further refinement of this principle has led to successful imaging equipment for OEID pixels [12, 17-19].

OEID are semiconductor instruments that can detect infrared radiation of various wavelengths during the manufacturing process[20]. OEID have been implemented successfully using mainly GaAs, InGaAs, and SiGe for mid-wave and long-wave infrared (IR)[21-25]. Besides, OEIDs are used for large infrared imaging system focal plane arrays. The idea of an integrated OEID for transforming FIR into NIR radiation has recently been proposed and implemented. The photocurrent injected from the OEID is the source of NIR radiation from the active layer in this method. The photocurrent in the OEID is related to the photo-excitement of electrons (holes) from the boundary states in the continuum above the barriers due to FIR absorption. [26]. The direct coupling of the OEID to the active layer has many problems, such as responsiveness, sensitivity, and signal-to-radius efficiency[27] All such problems are referred to in a previous study [15]. However, the current research is concentrated on the optical characteristics of optoelectronic integration between OEID and active layer. The paper is structured as follows: Section 2 outlines the basic assumption and models. The study of the proposed models is discussed in Section 3. Section 4 discusses the key findings of the debate. Conclusions of the study are given in Section 5.

2. Principle and Basic Assumptions

A far-infrared (FIR) radiation image is converted into a uniformly distributed photoelectron current excited by its inter-subband transitions.[28]. Under forward bias, the OEID is run highly enough to trigger the active layer. The OEID stack resistance decreases with infrared (IR) lighting. Therefore, the active layer receives additional voltage, which increases the emission [29]. The photocurrent into the active part of the system is injected to produce a nonuniform NIR image[26, 28, 30]. The OEID converter consideration consists of a broad gap in the area of doped N+ emitter communication, a small gap of undoped N space layer that forms an emission barrier, a narrow gap of doped OEID of n+ type, and a large undoped N space layer (collector's barrier). [31]. Schemes of the OEID imaging system's structure and operating principle are referred to by Ryzhii et al. [12]. Its action is based on direct injection into the active region of carriers photoexcited by mid- or far-IR radiation in the OEID and subsequent emission of near-IR radiation[27, 32]. An OEID thus acts as an FIR to NIR radiation converter, or as an optical output OEID. This system enables the IR and thermal imaging of Si-based charge-coupled devices (CCD) or CMOS cameras to work. GaAs is presumed to be the OEID active zone. A very high likelihood of band-to-band radiative

recombination enabling the development of high-efficiency optoelectronic emitters is a significant feature of GaAs and related compounds. [27]. The OEID efficiency is presumed to be limited in both the OEID and active sections by the electron injection from the OEID emitter and the lateral spreading of the photoelectrons. The electron injection current is also activated by the potential redistribution associated with FIR radiation absorption. Due to the equipotentiality of the OEID, the lateral distribution of the injected current is uniform. The image contrast decreases this current [28]. However, the current of the electrons injected from the OEID emitter may be low compared to the photoelectrons' current in OEID devices with a sufficient number of OEID layers. As a consequence, the current output emits nonuniform NIR radiation. [26, 28]. The photoelectrons' lateral diffusion in the OEID is also believed to be ignored with short transit time under high bias voltages [28]. The potential consequences of interface roughness is ignored in this study. One of the main advantages of the current study is the possibility of wavelength conversion of high energy radiation to another form.

3. Models Analysis OEID

3.1 Carriers concentration model of OEID

The OEID analytical model includes a diffusion equation that considers both photoelectron rebalancing and reabsorption[28]. Due to a concentration gradient of carriers, the current can be formed in semiconductors. In this case, the current is called the diffusion current [33]. In addition to this formula, is a definition of NIR radiation distribution throughout the active region[28]. The spatial distribution of electrons from OEID into the active layer is calculated by[12]

$$\frac{d^2\Sigma(x)}{dx^2} - \frac{\Sigma(x)}{l_D^2} + \frac{1}{D} \left(\frac{J(x)}{e} + \Gamma W \alpha_\Omega S_\Omega(x) \right) = 0 \quad (1)$$

where e denotes the electron charge, D is Injected photo-carrier diffusion coefficient, l_D represent the injected electrons diffusion length, Γ is the confinement factor, W is OEID portion of the device's thickness, α_Ω denote the interband absorption ratio of the inter-layer and active layer material, and S_Ω is Net NIR intensity which represents the propagation of trapped photons along the axis x . The injected electrons diffusion length can be described by

$$l_D = \sqrt{D\tau_1} \quad (2)$$

where τ_1 is the injected electrons net lifetime in the active layer, which can be described by[12]

$$\tau_1 = \frac{\tau_r \tau_n}{\tau_r + \tau_n} \quad (3)$$

where τ_n and τ_r denote the nonradiative lifetime and the radiative lifetime of electrons, respectively. Also, the confinement factor can be expressed by [12]

$$\Gamma = \frac{d_{Active}}{W} = \frac{d_{Active}}{d_{OEID} + d_{Active}} \quad (4)$$

where d_{OEID} and d_{Active} denote the OEID thicknesses and device portions, respectively. The thicknesses of the OEID obeys the equation [12]

$$d_{OEID} \square (N + 1)L \quad (5)$$

Where L and N denote the OEID structure period and the number of the layers, respectively. The net NIR intensity of the trapped photons that propagate back and forth along axis x can be represented by

$$S_{\Omega}(x) = S_{\Omega 0} + S_{\Omega q} e^{iqx} \quad (6)$$

Where q is the wavenumber that characterizes the MIR image's nonuniformity scale and the x -axis in the plane is directed. The photocurrent density can be presented by [34]

$$J(x) = J_0 + J_q e^{iqx} \quad (7)$$

The third term on the left side of Eq (1) is correlated with electrons' OEID injection. However, because of the absorption of the NIR photons emitted beyond the critical angle cone, the fourth term on the left-hand side of Eq (1) is connected to the recreation of the electron-hole pairs in the active region. These photons are trapped between the OEID's reflecting surfaces. The boundary conditions for solving Eq. (1) is

$$\left. \frac{d\Sigma}{dx} \right|_{x=\pm L} = 0 \quad (8)$$

Therefore, a formula is deduced and expressed to concentrate injected electrons in the active layer.

3.2 Image contrast transfer characteristics

The output of the OEID imager can be represented by the features of contrast (modulation) transfer that are defined by [26, 34]

$$\kappa(q) = \frac{I_{\Omega q} / I_{\Omega 0}}{I_{\omega q} / I_{\omega 0}} = \kappa_{OEID}(q) \cdot \kappa_{Active}(q) \quad (9)$$

where $I_{\omega q}$ and $I_{\omega 0}$ represent The FIR spatial signal amplitude (image), and the uniform FIR radiation

component. However, $I_{\Omega q}$ and $I_{\Omega 0}$ are the signal and uniform spatial distribution components of the NIR output photons. Also, the parameters $\kappa_{OEID}(q)$ and $\kappa_{Active}(q)$ are the spreading factors of photocurrent within OEID structures, respectively. If there are sufficient numbers of layers, then $\kappa_{OEID}(q) = 1$. This is due to a slight rise in OEID for many layers. Consequently, the uniform current pumped by the emitter is much smaller than that produced by the photon flux signal [12, 26]. The spatial distribution of the NIR photon output is indicated by [12].

$$I_{\Omega}(x) = T(1 - \delta) \frac{\Sigma(x)}{\tau_r} \quad (10)$$

Where T and δ , $(1 - \delta)$ denote the significant coefficient of transmission for the untrapped photons of NIR that calculated by a mismatch of the refractive index at the interfaces of the active zone, the fraction of the NIR photons trapped in the active layer due to complete internal reflection and the critical angle cone, respectively. Eq. (10) is a function of the spatial distribution of the electrons' concentration injected from the OEID into the active layer. The spatial distribution of the output NIR photons can also be expressed by another formula [34].

$$I_{\Omega}(x) = I_{\Omega 0} + I_{\Omega q} e^{iqx} \quad (11)$$

However, the injected electrons' concentration in the active layer can be given by [26, 34].

$$\Sigma(x) = \Sigma_0 + \Sigma_q e^{iqx} \quad (12)$$

Where Σ_0 and Σ_q in the active layers are the uniform and signal components of the electron concentration, the deduced Eq. (9) has been contrasted with Eq. (13), acquiring the uniform electron concentration and signal components in the active layer. Therefore, formulas for the uniform and signal spatial propagation components of the NIR output photons are obtained by substituting Eq. (13) from Eq. (11) and comparing the expression obtained with its analogs, Eq. (12). Such terms are provided by [26].

$$I_{\Omega 0} = T(1 - \delta) \frac{\Sigma_0}{\tau_r} \quad (13)$$

$$I_{\Omega q} = T(1 - \delta) \frac{\Sigma_q}{\tau_r} \quad (14)$$

A term for the characteristics of image contrast (modulation) transition is proposed and formulated by substitution from Eqs. (13-14) in Eq. (9).

4. RESULTS AND DISCUSSION

4.1 Concentration of the Carrier

The distribution of the NIR photons output depends on the concentration of the carrier. The carrier's concentration against the wave number at different numbers of layers and the span of the OEID structure is shown in Figs. (1-2), respectively. From these figures, the carrier concentration is found to be 5213.6cm^3 at uniformity image distribution with $q=0$. However, the carrier concentration increases with the wavenumber until a threshold limit. Then, it starts to decrease with wavenumber due to the non-uniformity distribution of the incident FIR image. It is also noted that the number of confined electrons within layers increases with the number of layers. Therefore, the spatial distribution of the electrons concentration injected from the OEID into the active layer increases, as shown in Fig. (3). With the OEID structure period, however, the number of dissipated electrons increases. Therefore, electron containment is diminishing. Thus, the electrons' spatial distribution injected into the active layer from the OEID decreases, as shown in Fig. (4).

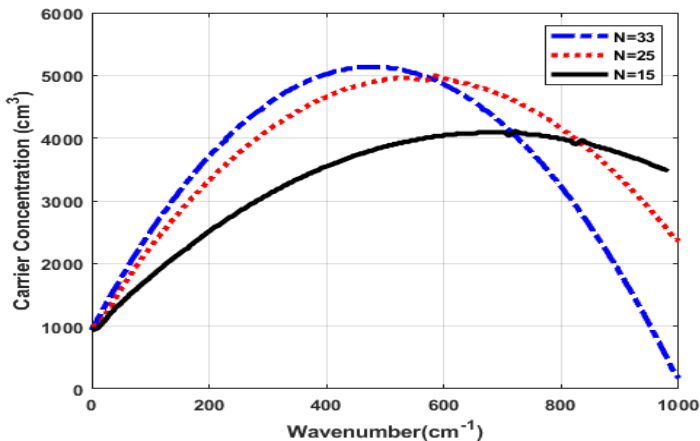


Fig. (1): Wave number Carrier concentration at various QWs

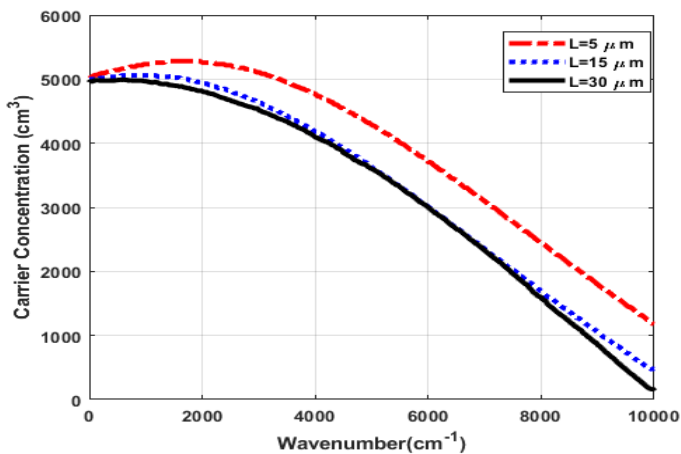


Fig. (2): Wave Number Carrier Concentration for various structure lengths

4.2 Contrast transfer characteristics

Figures (3-6) show the dependence of contrast transfer function on the wave number of image nonuniformity for devices with different lifetime ratios (τ_1/τ_r), number of layers, and a period of the OEID structure, and thicknesses of the active portions of the device, respectively. From these figures, the nonuniformity of incident FIR radiation increases the nonuniform photocurrent. However, the injection of nonuniformly distributed photocurrent into the active region introduces a nonuniform NIR image. Therefore, the contrast transfer characteristics decrease with the nonuniformity wavenumber of the image. We observed that the contrast transfer function approaches its maximum value with $q=0$. However, the effects of the underlined parameters vanish at $q=0$.

The contrast transfer function increases with the time ratio (τ_1/τ_r) as illustrated in Fig. (3). The recycling of NIR photons emitted by has negative effects on the operation of OEID image devices. Hence, the electrons injected into the are thermionic due to the strong electric field applied across the OEID. Therefore, a little radiative recombination of electrons is introduced. Thus, the lifetime ratio (τ_1/τ_r) is increased. Hence, the contrast transfer function is decreased. On the other hand, the lifetime ratio (τ_1/τ_r) is reduced with radiative recombination. The radiative recombination between electrons and holes within the active region increases due to little trapping of electron charges inside the inter-band.

Moreover, the contrast transfer function is improved with the decrease of layers, as illustrated in Fig. (4). The applied electric field increases with the number of layers within OEID structure. Hence, the electrons inside layer bound states are photoexcited. Consequently, the probability of reabsorption of photons increases. Therefore, the image contrast function is decreased.

The contrast transfer function is increased with the OEID structure period, as depicted in Fig. (5). The numbers of photoexcited carriers are increasing with the period of OEID under incident FIR radiation. Consequently, these carriers are injected into the active region to generate radiative recombination. Hence, the contrast transfer function is increased.

The contrast transfer function increases with the thicknesses of the portions of the device, as shown in Fig. (6). This is due to the increase of the uniform electron concentration within an active region with the thicknesses of the portions of the device. Thus, the contrast transfer function is increased. The optimized parameters of OEID are shown in Table (1).

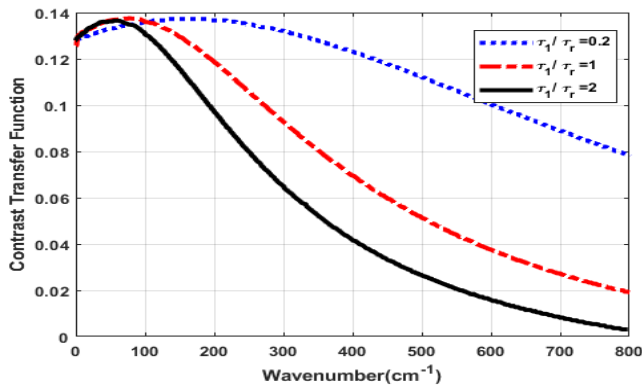


Fig. (3): Wave number comparison feature at various lifetime ratios

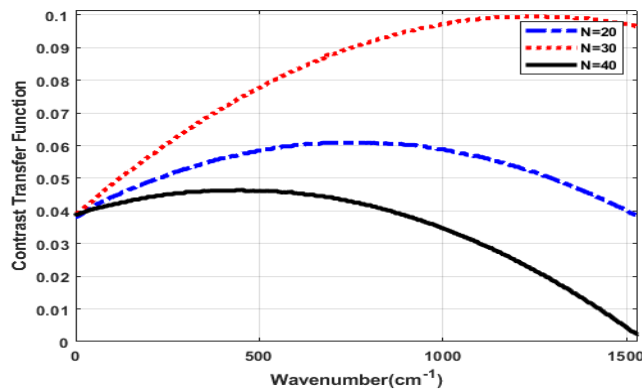


Fig. (4): Wave number comparison transmission function at various layers

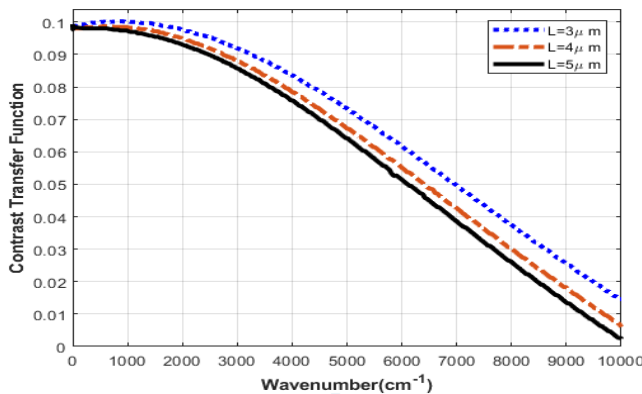


Fig. (5) Wave number comparison function for different length of the OEID structure

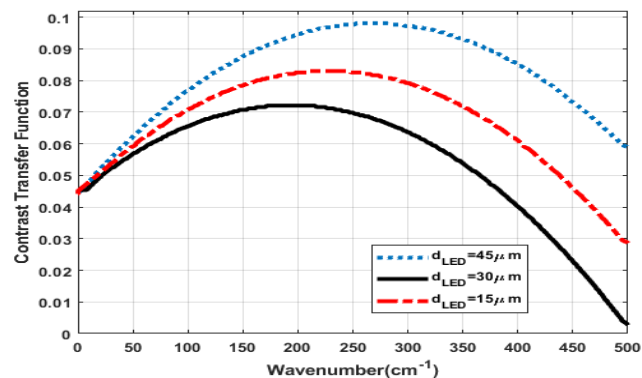


Fig. (6): Wave number contrasting feature at various thicknesses of the active layers

Table (1): Parameters optimization

Parameters	d (m)	d _{Active} (m)	N	q
Values	0.0123	0.0016	13	0.206

5. CONCLUSION

The optical characteristics of the OEID for imaging conversion purposes are the main target of this research. Hence, this paper discusses the FIR image conversion to NIR pixelless imaging of OEID optoelectronic device. MATLAB environment is used to discuss the characteristics of this instrument. Therefore, the study aims to study and evaluate the characteristics of the converted image. These image characteristics are carriers concentration and contrast transfer function. Therefore, proposed explicit solutions are investigated. The influence of photons recycling problems on the underlined OEID structure is addressed. Moreover, the uniform and nonuniform imaging effects on the image characteristics are presented. Consequently, parameter optimizations of OEID structure are estimated. The results show that the concentration of the carrier changes the behaviors of the NIR image production. The achieved results show that the uniformity of the image reduces the characteristics of contrast transfer. But its maximum value at $q=0$ is approached. Furthermore, with the recombination of the carrier within the active layer structure, the image resolution is decreased. The image conversion performance level has degraded significantly. The inference is that the long OEID duration affects the contrast transfer and image resolution behaviors. The best value of the concentration of the sheet donor has been found. The results obtained confirm the possible applicability for image conversion under various parameter conditions for proposed OEID models.

REFERENCES

- [1] I. Yang, S. Kim, M. Niihori, A. Alabadla, Z. Li, L. Li, et al., "Highly uniform InGaAs/InP quantum well nanowire array-based light emitting diodes," *Nano Energy*, vol. 71, p. 104576, 2020/05 2020.
- [2] A. F. Benner, M. Ignatowski, J. A. Kash, D. M. Kuchta, and M. B. Ritter, "Exploitation of optical interconnects in future server architectures," *IBM Journal of Research and Development*, vol. 49, pp. 755-775, 2005.
- [3] Y. Zhu, S. Noda, and A. Sasaki, "Theoretical analysis of transient behavior of optoelectronic integrated devices," *IEEE Transactions on Arab J. Nucl. Sci. Appl.*, Vol. 54, 3, (2021)

- Electron Devices, vol. 42, pp. 646-651, 1995/04 1995.
- [4] Y. Zebda, M. Khodier, and B. Darwish, "Transient response of optoelectronic integrated bistable device," *IEEE Transactions on Electron Devices*, vol. 45, pp. 85-90, 1998.
- [5] I. Yang, S. Kim, M. Niihori, A. Alabadla, Z. Li, L. Li, et al., "Highly uniform InGaAs/InP quantum well nanowire array-based light emitting diodes," *Nano Energy*, vol. 71, 2020.
- [6] V. Ahmadi and M. H. Sheikhi, "Numerical analysis for the characteristics of a QW-structure optoelectronic integrated device," presented at the ICSE'98. 1998 IEEE International Conference on Semiconductor Electronics. Proceedings (Cat. No.98EX187), 1998.
- [7] X. Huang, X. Feng, L. Chen, L. Wang, W. C. Tan, L. Huang, et al., "Fabry-Perot cavity enhanced light-matter interactions in two-dimensional van der Waals heterostructure," *Nano Energy*, vol. 62, pp. 667-673, 2019/08/01/ 2019.
- [8] J. Jiang, Q. Wang, B. Wang, J. Dong, Z. Li, X. Li, et al., "Direct lift-off and the piezo-phototronic study of InGaN/GaN heterostructure membrane," *Nano Energy*, vol. 59, pp. 545-552, 2019/05/01/ 2019.
- [9] D. H. Jung, J. H. Park, H. E. Lee, J. Byun, T. H. Im, G. Y. Lee, et al., "Flash-induced ultrafast recrystallization of perovskite for flexible light-emitting diodes," *Nano Energy*, vol. 61, pp. 236-244, 2019/07/01/ 2019.
- [10] S. Jit and B. B. Pal, "A new optoelectronic integrated device for light-amplifying optical switch (LAOS)," *IEEE Transactions on Electron Devices*, vol. 48, pp. 2732-2739, 2001.
- [11] E. Darabi, V. Ahmadi, and K. Mirabbaszadeh, "Analysis for the characteristics of a voltage tunable functional quantum structure optoelectronic integrated device," presented at the Proceedings of CAOL 2005. Second International Conference on Advanced Optoelectronics and Lasers, 2005., 2005.
- [12] V. Ryzhii and H. C. Liu, "Photonic breakdown in up-conversion imaging devices based on the integration of quantum-well infrared photodetector and light-emitting diode," *Journal of Applied Physics*, vol. 92, pp. 2354-2358, 2002.
- [13] W. Lv, J. Zhong, Y. Peng, Y. Li, X. Luo, L. Sun, et al., "Organic near-infrared upconversion devices: Design principles and operation mechanisms," *Organic Electronics*, vol. 31, pp. 258-265, 2016/04 2016.
- [14] Y. Yang, Y. H. Zhang, W. Z. Shen, and H. C. Liu, "Semiconductor infrared up-conversion devices," *Progress in Quantum Electronics*, vol. 35, pp. 77-108, 2011.
- [15] S. U. Eker, Y. Arslan, M. Kaldirim, and C. Besikci, "QWIP focal plane arrays on InP substrates for single and dual band thermal imagers," *Infrared Physics & Technology*, vol. 52, pp. 385-390, 2009/11 2009.
- [16] V. Ryzhii, I. Khmyrova, and S. Oktyabrsky, "Device Model of Integrated QWIP-HBT-LED Pixel for Infrared Focal Plane Arrays," presented at the 32nd European Solid-State Device Research Conference, 2002.
- [17] M. Abdi-Jalebi, Z. Andaji-Garmaroudi, S. Cacovich, C. Stavarakas, B. Philippe, J. M. Richter, et al., "Maximizing and stabilizing luminescence from halide perovskites with potassium passivation," *Nature*, vol. 555, pp. 497-501, 2018/03 2018.
- [18] T. Jeon, S. J. Kim, J. Yoon, J. Byun, H. R. Hong, T.-W. Lee, et al., "Hybrid Perovskites: Effective Crystal Growth for Optoelectronic Applications," *Advanced Energy Materials*, vol. 7, p. 1602596, 2017/05/24 2017.
- [19] H. Palneedi, J. H. Park, D. Maurya, M. Peddigari, G.-T. Hwang, V. Annapureddy, et al., "Laser Processing of Metal Oxides: Laser Irradiation of Metal Oxide Films and Nanostructures: Applications and Advances (Adv. Mater. 14/2018)," *Advanced Materials*, vol. 30, p. 1870094, 2018/04 2018.
- [20] A. C. P. Mazzetti, "Current noise in quantum well infrared photodetectors: effect of electron Coulomb interaction," *Philosophical Magazine B*, vol. 80, pp. 775-780, 2000/04/01 2000.
- [21] D. Z. Ting, A. Soibel, S. A. Keo, S. B. Rafol, J. M. Mumolo, J. K. Liu, et al., "Development of quantum well, quantum dot, and type II superlattice infrared photodetectors," *Journal of Applied Remote Sensing*, vol. 8, p. 084998, 2014/02/19 2014.

- [22] M. Naser, M. J. Deen, and D. A. Thompson, "Modeling and Optimization of Quantum Dot Infrared Photodetectors," presented at the 214th ECS Meeting, Honolulu, 2019.
- [23] M. S. El-Tokhy and I. I. Mahmoud, "Performance evaluation of quantum well infrared phototransistor instrumentation through modeling," *Optical Engineering*, vol. 53, pp. 054104-054104, 2014.
- [24] Z. Li and Y. Ye, "Chapter 7 - Two-dimensional materials," in *Nanoscale Semiconductor Lasers*, C. Tong and C. Jagadish, Eds., ed: Elsevier, 2019, pp. 165-189.
- [25] Y. Wan, J. Norman, and J. Bowers, "Chapter Nine - Quantum dot microcavity lasers on silicon substrates," in *Semiconductors and Semimetals*. vol. 101, S. Lourduoss, J. E. Bowers, and C. Jagadish, Eds., ed: Elsevier, 2019, pp. 305-354.
- [26] V. Ryzhii, I. Khmyrova, and P. Bois, "Photon mechanism of image smearing in integrated QWIP-LED pixelless devices," *IEEE Journal of Quantum Electronics*, vol. 35, pp. 1693-1696, 1999.
- [27] S. Oktyabrsky, I. Khmyrova, and V. Ryzhii, "Characteristics of integrated QWIP-HBT-LED up-converter," *IEEE Transactions on Electron Devices*, vol. 50, pp. 2378-2387, 2003/12 2003.
- [28] I. Khmyrova, P. Bois, and V. Ryzhii, "Electron spreading effects in quantum well pixelless imagers," *Physica B: Condensed Matter*, vol. 272, pp. 502-504, 1999.
- [29] E. Dupont, M. Byloos, T. Oogarah, M. Buchanan, and H. C. Liu, "Optimization of quantum-well infrared detectors integrated with light-emitting diodes," *Infrared Physics & Technology*, vol. 47, pp. 132-143, 2005/10 2005.
- [30] S. Chiu; and E. Dupont, "Image smearing in a quantum well infrared photodetector integrated with a light emitting diode," 1998.
- [31] V. Ryzhii, I. Khmyrova, M. Ershov, M. Ryzhii, and T. Iizuka, "Theoretical study of an infrared-to-visible wavelength quantum-well converter," *Semiconductor Science and Technology*, vol. 10, pp. 1272-1276, 1995/09/01 1995.
- [32] M. Ershov, H. C. Liu, and L. M. Schmitt, "Image transformation in integrated quantum well infrared photodetector-light emitting diode," *Journal of Applied Physics*, vol. 82, pp. 1446-1449, 1997/08 1997.
- [33] M. S. El_Tokhy and I. I. Mahmoud, "Performance analysis of PIN photodiode under gamma radiation effects through modeling," *Journal of Optics*, vol. 44, pp. 353-365, 2015/11/06 2015.
- [34] V. Ryzhii and I. Khmyrova, "Electron and photon effects in imaging devices utilizing quantum dot infrared photodetectors and light-emitting diodes," presented at the *Photodetectors: Materials and Devices V*, 2000.